

UNCLASSIFIED

AD NUMBER
AD883322
NEW LIMITATION CHANGE
TO Approved for public release, distribution unlimited
FROM Distribution authorized to U.S. Gov't. agencies only; Test and Evaluation; APR 1971. Other requests shall be referred to Naval Ship Research and Development Center, Washington, DC 20034.
AUTHORITY
NSRDC ltr dtd 19 Mar 1974

THIS PAGE IS UNCLASSIFIED

Report 3374

HYDRODYNAMIC PERFORMANCE OF A PROPOSED CRUISING, DUCTED PROPELLER FOR SUBMARINES

AD 883322

AD No.
TTC FILE COPY

NAVAL SHIP RESEARCH AND DEVELOPMENT CENTER

Washington, D.C. 20034



2

HYDRODYNAMIC PERFORMANCE OF A PROPOSED CRUISING, DUCTED PROPELLER FOR SUBMARINES

by

John L. Beveridge

Distribution limited to U.S. Government agencies only;
Test and Evaluation; 28 Nov 1970. Other requests for
this document must be referred to NSRDC, Code 500.

SHIP PERFORMANCE DEPARTMENT
RESEARCH AND DEVELOPMENT REPORT

DDC
RECEIVED
MAY 10 1971
REGULATED

April 1971

Report 3374

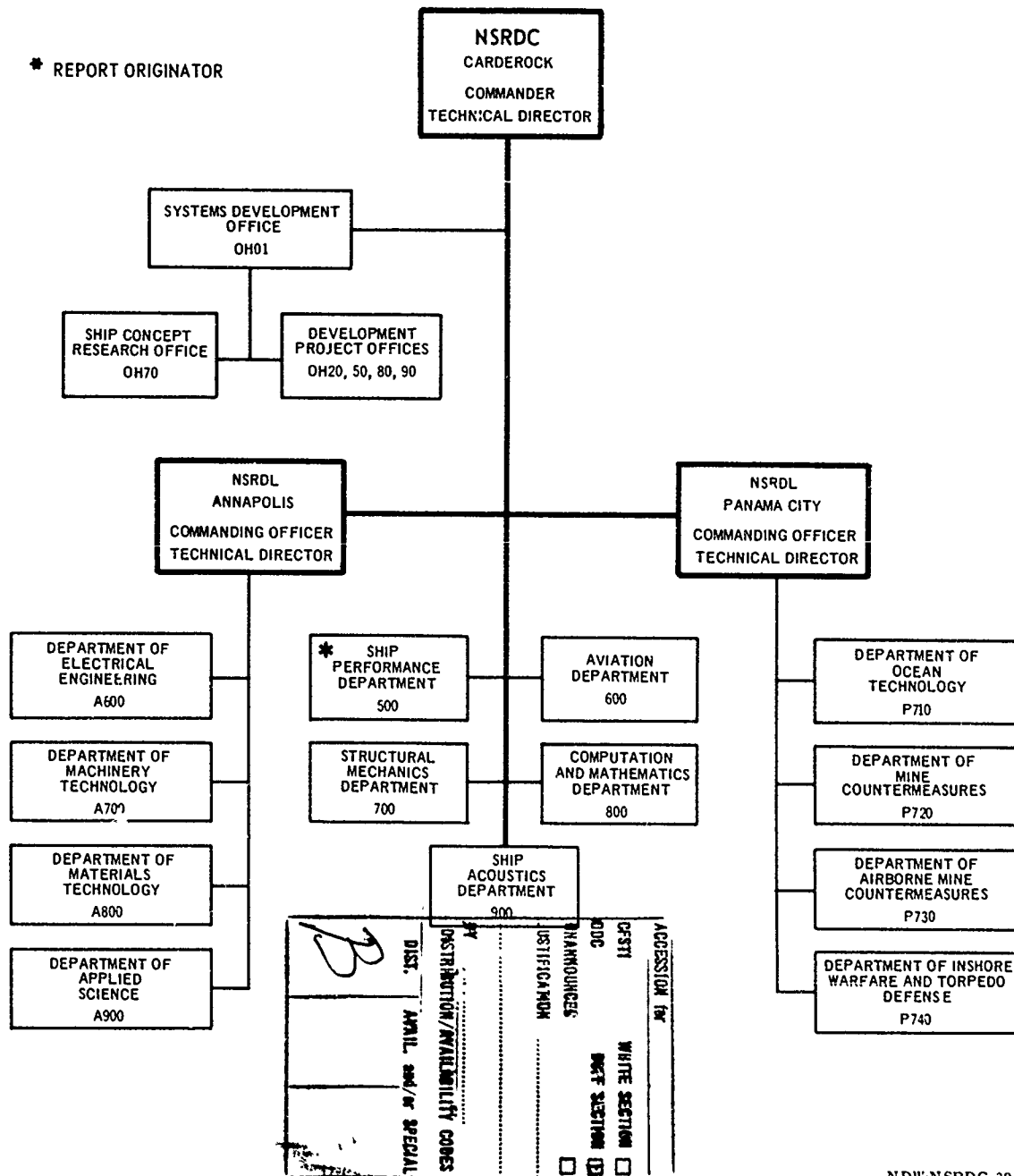
B - 1/3

The Naval Ship Research and Development Center is a U.S. Navy center for laboratory effort directed at achieving improved sea and air vehicles. It was formed in March 1967 by merging the David Taylor Model Basin at Carderock, Maryland and the Marine Engineering Laboratory (now Naval Ship R & D Laboratory) at Annapolis, Maryland. The Mine Defense Laboratory (now Naval Ship R & D Laboratory) Panama City, Florida became part of the Center in November 1967.

Naval Ship Research and Development Center
Washington, D.C. 20034

MAJOR NSRDC ORGANIZATIONAL COMPONENTS

* REPORT ORIGINATOR



DIST. APRIL 1967
 DISTRIBUTION/AVAILABILITY CODES
 BY
 AUTHORITY
 ANNOUNCES
 JUSTIFICATION
 ACCESSION NO.
 CEPTI
 W/TE SECTION
 DOC
 DIST SECTION ID

DEPARTMENT OF THE NAVY
NAVAL SHIP RESEARCH AND DEVELOPMENT CENTER
WASHINGTON, D.C. 20034

HYDRODYNAMIC PERFORMANCE OF A PROPOSED CRUISING,
DUCTED PROPELLER FOR SUBMARINES

by

John L. Beveridge

Distribution limited to U.S. Government agencies only;
Test and Evaluation; 28 Nov 1970. Other requests for
this document must be referred to NSRDC, Code 500.

April 1971

Report 3374

TABLE OF CONTENTS

	Page
ABSTRACT	1
ADMINISTRATIVE INFORMATION	1
INTRODUCTION	1
GEOMETRY	2
HULL	2
DUCT AND PROPELLER	2
APPROACH	4
DESIGN INFORMATION	5
COMPUTER PROGRAMS	5
PROCEDURE AND NUMERICAL DATA	5
THEORETICAL PERFORMANCE	6
DUCT PRESSURE DISTRIBUTION	6
EFFICIENCY OF DUCT AND PROPELLER SYSTEM	7
PROPULSION TEST RESULTS AND DISCUSSION	8
CONCLUSIONS	11
ACKNOWLEDGMENTS	11
REFERENCES	22

LIST OF FIGURES

Figure 1 – NSRDC Model 4620 with Ducted Propeller 4271	12
Figure 2 – Comparison of Hull Shapes for NSRDC Model 4620 and for the Point Source and Line Sink of Reference 1	13
Figure 3 – Cruising Duct 2.1	13
Figure 4 – Duct Section and Dimensions	14
Figure 5 – Details of Propeller 4271	14
Figure 6 – Hull Wake and Total Wake of Hull Plus Duct	15
Figure 7 – Additional Angles of Attack for Blade Sections of Propeller 4271	16

	Page
Figure 8 – Final Blade-Pitch Distribution for Propeller 4271	17
Figure 9 – Pressure Distribution on Duct	18
Figure 10 – Ducted Propeller Efficiencies versus RPM	19
Figure 11 – Model 4620 Overload and Underload Propulsion with Ducted Propeller 4271	20
Figure 12 – Power and RPM Curves for a 200-Foot Prototype of Model 4620	21

LIST OF TABLES

Table 1 – Offsets and Particulars for NSRDC Model 4620	3
Table 2 – Duct Camber Ordinates	4
Table 3 – Comparative Propulsion Data for a 200-Foot Prototype of Model 4620 at $V = 29.3$ knots	9

NOTATION

A_e	Propeller expanded-blade area
A_0	Propeller disk area
C_p	Pressure coefficient p/q
C_{P_s}	Propeller power coefficient $P_D / \frac{1}{2} \rho A_0 V^3$
C_T	Total resistance coefficient $R_T / \frac{1}{2} \rho S V^2$
$(C_{Th})_s$	Propeller thrust-loading coefficient $T_p / \frac{1}{2} \rho A_0 V^2$
C_{TP}	Propeller thrust-power coefficient $T_p V_a / \frac{1}{2} \rho A_0 V^3$
c	Duct chord length
D	Propeller diameter or maximum diameter of a body of revolution
J_s	Propeller advance coefficient V / nD
L	Body length
ℓ	Propeller blade section length
n	Propeller rate of revolution in rps
P	Propeller geometric pitch
P_D	Power delivered to propeller $2 \pi Qn$
P_E	Effective (tow rope) power $R_T V$
p	Local static pressure, excluding hydrostatic pressure
Q	Propeller torque
q	Free-stream stagnation pressure $\frac{1}{2} \rho V^2$
R	Propeller radius or radius in general
R_T	Total resistance
rpm	Propeller revolutions per minute
r_s	Camber offset, measured from duct axis
S	Wetted surface
shp	Shaft horsepower

T	Thrust		
t	Thrust-deduction coefficient		
V	Ship speed		
V_a	Speed of advance $(1 - w_0)V$, includes hull and duct velocities where appropriate		
V_x	Axial component of local velocity, includes hull and duct velocities where appropriate		
$1 - w_0$	Propeller effective inflow velocity ratio V_a / V		
$1 - w_x$	Propeller local inflow velocity ratio V_x / V		
X	Axial coordinate, origin at bow for hull, at leading edge for duct		
x_c	Nondimensional duct length		
x	Propeller radius fraction or nondimensional length		
Y	Offset of meridian profile for body of revolution		
y	Nondimensional offset Y / D		
Z	Number of propeller blades		
α_i^0	Ideal angle of attack due to loading in degrees		
α_t^0	Angle of attack due to thickness in degrees		
β_i	Hydrodynamic pitch angle		
ϵ	Section ratio of drag to lift		
η_B	Propeller efficiency C_{TP} / C_{Ps} , Equation (6)		
η_D	Quasi propulsive coefficient P_E / P_D		
η_H	Hull efficiency $(1 - t) / (1 - w_0)$		
η_T	Total efficiency of duct plus propeller $\eta_B [1 + (T_d) / (T_p)]$		
ρ	Mass density		
Subscripts			
d	Duct	s	Ship speed
h	Propeller hub	Q	Source
v	Nonviscous	B	Sink
p	Propeller		

ABSTRACT

A theoretical and experimental investigation was performed to determine the steady-state propulsion characteristics of a cruising, ducted-propeller system for a submersible body of revolution. The most important aspects of the design method and numerical procedures are discussed. The theoretically predicted and experimental performance of the ducted propeller showed good agreement on power. However the experimental rpm was 6 percent higher than predicted; this difference is attributed to the fact that the propeller was underpitched due to an error in input to the computer program. The subject propulsion system was found to be less efficient than an optimum unshrouded, wake-adapted propeller, but the optimum rpm-diameter relationship was not determined for the ducted propeller. ()

ADMINISTRATIVE INFORMATION

The work was authorized under the Naval Ship Systems Command General Hydro-mechanics Research Program and was funded under Subproject SR009-0101, Task 0101.

INTRODUCTION

Ducted propellers offer an alternative propulsion system to conventional stern propellers for ships and submarines. Specific types of ducted propellers have been used, depending on the design conditions to be met. Kort nozzle and pumpjet designs are well-known examples of flow-accelerating and flow-decelerating types, respectively. The primary objective of the present investigation was to study the feasibility of using a so-called cruising, ducted-propeller propulsion system on a high-speed submarine. Kriebel and Mendenhall¹ have made a theoretical analysis of the flow over an underwater hull (the same hull form is treated in this report) with a stern-mounted ducted propeller (flow accelerating duct). The optimum duct camber (largest duct thrust without duct flow separation) derived in Reference 1 was used in conjunction with the Morgan² ducted-propeller theory and a computer program reported by Caster³ to design and predict the performance of a cruising, ducted propeller.

A cruising, ducted propeller can be loosely defined in terms of the shape of the duct-mean camber, that is, a camber with the following properties:

1. No leading edge suction.
2. No hull-duct interference (no "thrust deduction") except that due to the propeller.
3. Maximum duct thrust at the onset of separation.

¹References are listed on page 22.

If a ducted propeller possessing these properties can be designed to compare favorably with the propulsive efficiency of an unshrouded stern-mounted propeller, then other possible advantages can be utilized without penalty in absorbed power. It is visualized that the stern control surfaces (rudders and diving planes) would be mounted externally on the duct. Possible collateral benefits include (1) a reduction in noise generation and induced vibration of the hull and (2) an added stabilizing-fin effect from the duct. This report presents and discusses the theoretical design techniques and the experimental results used in a hydrodynamic evaluation of an optimum cruising, ducted propeller on NSRDC Hull Model 4620.⁴

GEOMETRY

HULL

NSRDC Model 4620 is a 15.0-ft submersible hull (free-flooding) constructed of fiberglass and equipped with standard NSRDC instrumentation for measuring body, duct, and propeller forces. Table 1 gives the offsets and principal dimensions of the model hull. Figure 1 shows several views of the model with the ducted propeller mounted in place for testing.

Reference 1 approximated the profile of the body-of-revolution hull by a point-source, line-sink distribution. The strength of the line sink was assumed to be affine to the slope of the hull sectional area curve. Since the singularities used to generate the hull shape are an important part of the analytical derivation of the duct camber, it is interesting to compare the hull shape for a point source and line sink with that of NSRDC Model 4620. Note in Figure 2 that the chosen singularity system accurately approximated the actual hull shape in the vicinity of the duct. The analysis of Reference 1 was insensitive to the shape of the bow portion of the hull.

DUCT AND PROPELLER

Figure 3 shows the aluminum duct. An exploded view is included to show the various components of the ducted propeller; major features include propeller, cruciform supporting struts, and the "backbone element," which contains propeller-shaft bearings and differential-reluctance block gages for measuring the duct axial force. Transparent plastic windows were provided in the duct surface for viewing the propeller, should cavitation tests be performed.

Duct camber ordinates are given in Table 2. The NACA 16-009 thickness form was added to the camber to obtain the duct section. The resulting section is shown in Figure 4 together with pertinent duct dimensions.

Figure 5 shows seven-bladed Propeller 4271 which was designed for the duct. Expanded blade-section lengths were calculated from the relation

$$\ell/D = \frac{(\pi/3) \frac{A_e}{A_0}}{Z(1-x_h)} \left[1 + \frac{x-x_h}{1-x_h} \right]$$

TABLE 1

Offsets and Particulars for NSRDC Model 4620

x	X inches	y	Y inches
0.00	000.0	0.0000	0.000
0.02	3.6	0.1427	3.500
0.04	7.2	0.2029	4.977
0.06	10.8	0.2490	6.108
0.08	14.4	0.2873	7.047
0.10	18.0	0.3200	7.850
0.12	21.6	0.3485	8.549
0.14	25.2	0.3734	9.160
0.16	28.8	0.3953	9.697
0.18	32.4	0.4145	10.17
0.20	36.0	0.4312	10.58
0.22	39.6	0.4457	10.93
0.24	43.2	0.4581	11.24
0.26	46.8	0.4687	11.50
0.28	50.4	0.4775	11.71
0.30	54.0	0.4848	11.89
0.32	57.6	0.4905	12.03
0.34	61.2	0.4947	12.13
0.36	64.8	0.4977	12.21
0.38	68.4	0.4994	12.25
0.40	72.0	0.5000	12.27
0.42	75.6	0.4995	12.25
0.44	79.2	0.4979	12.21
0.46	82.8	0.4953	12.15
0.48	86.4	0.4917	12.06
0.50	90.0	0.4878	11.97
0.52	93.6	0.4818	11.82
0.54	97.2	0.4755	11.66
0.56	100.8	0.4684	11.49
0.58	104.4	0.4603	11.29
0.60	108.0	0.4513	11.07
0.62	111.6	0.4414	10.83
0.64	115.2	0.4305	10.56
0.66	118.8	0.4187	10.27
0.68	122.4	0.4058	9.954
0.70	126.0	0.3919	9.613
0.72	129.6	0.3768	9.243
0.74	133.2	0.3605	8.843
0.76	136.8	0.3429	8.411
0.78	140.4	0.3239	7.945
0.80	144.0	0.3036	7.447
0.82	147.6	0.2817	6.910
0.84	151.2	0.2582	6.334
0.86	154.8	0.2330	5.715
0.88	158.4	0.2060	5.053
0.90	162.0	0.1771	4.344
0.92	165.6	0.1461	3.584
0.94	169.2	0.1131	2.774
0.96	172.8	0.0778	1.908
0.98	176.4	0.0401	0.984
1.00	180.0	0.0000	0.000

Formula:

$$y^2 = a_1x + a_2x^2 + a_3x^3 + a_4x^4 + a_5x^5 + a_6x^6$$

where:

$$a_1 = 1.000000$$

$$a_2 = 1.137153$$

$$a_3 = -10.774885$$

$$a_4 = +19.784286$$

$$a_5 = -16.792534$$

$$a_6 = + 5.645977$$

Wetted Surface Coefficient = 0.7324

$$LCB, \bar{x} = 0.4456$$

$$L/D = 7.339$$

Model Particulars:

Length, ft = 15.0000

Diameter, ft = 2.044 (24.53 in.)

Nose Radius, ft = 0.1392 (1.670 in.)

Tail Radius, ft = 0.0000

Wetted Surface, ft² = 70.55Volume, ft³ = 29.53

LCB, ft = 6.6840

Ship Particulars:

L = 200 ft

D = 27 ft 3 in.

where

- l is section length,
- D is propeller diameter,
- A_e is the expanded area of all blades,
- A_0 is the propeller disk area,
- x is the radius fraction,
- x_h is the radius fraction of the hub, and
- Z is the number of propeller blades.

The previous expression results in a wide tip propeller of the Kaplan type. A NSRDC modified-66-thickness form, cambered with an $a = 0.8$ mean line, was used for the blade sections.

TABLE 2
Duct Camber Ordinates

x/c	r_s/c
0.00	0.682
0.05	0.683
0.10	0.679
0.20	0.665
0.30	0.642
0.40	0.614
0.50	0.585
0.60	0.557
0.70	0.532
0.80	0.513
0.90	0.502
0.95	0.500
1.00	0.500

APPROACH

An optimum duct camber (Duct 2.1 of Reference 1) was specified. With the duct camber and duct size chosen, the problem was to design and predict the performance of the ducted propeller that absorbed minimum power at design thrust and speed. To solve the problem, the work of Morgan and Caster^{2,3,5} was used. The duct forces, circulation, pressure distribution, and the effect of the duct on the propeller were computed by the linearized theory of the duct presented by Morgan.² Propeller design and performance were based on the Lerbs lifting-line theory⁶ for moderately loaded, finite-bladed propellers. In determining the effect of the propeller on the duct, the average axial and radial velocity components induced on the duct by the propeller were obtained from a propeller actuator disk theory as developed by Hough and Ordway.⁷

As mentioned previously, the submersible hull form used for the study was identical to the model hull for which computations were performed in Reference 1. Experimental wake data, needed in the ducted-propeller design procedure, have been previously reported for the hull form used.⁴ Reference 3 contains a complete discussion of the form and nature of the input required for the ducted-propeller computer program, the various options available, the output provided, and the assumptions of and limitations to the theory. It seems desirable to restate here the most important assumptions and limitations:

- “1. The fluid is inviscid and incompressible and no separation occurs. . . . The viscous drag of the duct, which includes both the skin-friction and pressure drag, can also be calculated
- “2. The free-stream flow must be axisymmetric.
- “3. The duct is axisymmetric and of finite length.

“4. The duct can be represented mathematically by a distribution of ring vortices and ring sources along a cylinder of constant diameter. This implies that the boundary conditions are linearized.”

A parametric study was made to optimize propeller rpm for the given duct diameter. The optimum rpm-diameter relationship would normally be determined from a parametric study, but the more limited objective of evaluating the subject configuration was pursued in the present case. Although the Lerbs lifting-line propeller theory was used to design (in the sense of obtaining the best blade radial-loading distribution) and to predict the performance of a series of propellers, the final propeller design for optimum rpm was based on propeller lifting-surface theory (blade thickness included).

DESIGN INFORMATION

COMPUTER PROGRAMS

Three IBM-7090 computer programs were used to assist in the design, performance prediction, and analysis of the ducted-propeller propulsion system.

Program 1 was a composite program³ with several options which could be used either to predict the hydrodynamic characteristics of an axisymmetric duct (e.g., duct thrust and duct-pressure distribution) or to iterate a complete ducted-propeller design. Particularly useful were the options which permitted including input for an arbitrary axisymmetric velocity, including propeller (or otherwise) induced velocity at the duct surface, obtaining the ideal angle of attack of the duct section, and obtaining the velocity field inside the duct.

Program 2 was a lifting-line propeller program⁸ which was used (1) to find either the optimum or nonoptimum radial distribution of hydrodynamic pitch angle (to produce the design thrust or power) and (2) to predict propeller performance. The program provided the necessary input for the final propeller design by lifting-surface theory.

Program 3 was a composite design method^{9, 10} which was used to obtain the final pitch distribution and camber ratios for the propeller, based on lifting-surface theory with blade thickness included.

The following sections discuss how these various programs and options were used in the present analysis.

PROCEDURE AND NUMERICAL DATA

A thrust-loading coefficient $C_{T_{hs}} = T / \frac{1}{2} \rho A_0 V^2 = 0.40$ was used as specified in Reference 1 for design of the ducted system (duct loading and propeller loading relate to model scale). Duct boundary-layer characteristics and shear drag as well as hull resistance and wake data were calculated for the model range of Reynolds number.^{1,4}

With the duct geometry as input, Program 1 was used to obtain duct thrust, duct pressure distribution (discussed in the next section), and the axial component of the velocity

induced by the duct at the propeller plane. Figure 6 shows curves of the experimental wake⁴ for Model 4620 hull and the total propeller inflow (hull plus duct). The option of Program 1 which iterated a complete ducted-propeller design was used, in conjunction with Program 2 for a parametric study to optimize propeller rpm for the given diameter and thrust loading. The final propeller design (Figure 5) was then completed by using Program 3.

Some important aspects of the propeller-design method according to lifting surface theory will be briefly described. Essentially the study utilized a combination of work by Kerwin and Leopold,¹⁰ Pien,¹¹ and Cheng.⁹ The chordwise distribution of camber ratio was obtained for nine radii by the Pien mathematical model, which used a continuous distribution of vortices. The final pitch angle of each blade section was obtained by adding two angles of attack to the hydrodynamic pitch angle, the ideal angle of attack due to loading from lifting-surface theory, and an angle of attack due to blade thickness. The additional angles are shown in Figure 7, and the final pitch distribution is given in Figure 8.

THEORETICAL PERFORMANCE

DUCT PRESSURE DISTRIBUTION

Figure 9 is a composite graph which shows the variation of the theoretical pressure coefficient versus chordwise position x_c for points on the duct outside and inside surfaces. The curve shows the pressure distribution calculated by the present method for the final ducted-propeller configuration at optimum propeller rpm. Data points are shown for other conditions as follows:

1. Computed results given in Reference 1, based on a duct of zero thickness (indicated by \square and σ).
2. Results computed by the present method for the final configuration but assuming a duct of zero thickness (indicated by \circ and σ).

Results of the two approaches to a solution for the duct pressure distribution were in fairly good agreement for the last half of the duct length, particularly on the duct outside surface. As expected, the pressures calculated by the present method were usually closer, to the data of Reference 1 when duct thickness was zero. Integration of the present pressure distribution for zero duct thickness yielded a value of 0.06 for T_d/T_p . This compares to the value of 0.07 obtained in Reference 1, an insignificant difference. If thickness is included, $T_d/T_p = 0.04$.

An increasing pressure gradient with respect to x_c was indicated in the forebody region of the duct outside surface. This could lead to laminar separation with a consequent deterioration in duct performance; the increase in actual pressure drag would undoubtedly offset any reduction in the duct shear force. According to Reference 1, the transition from laminar to turbulent flow occurred at $x_c \approx 0.15$ at design condition on both the inside and outside duct surface. Theoretically, at design condition the flow is not separated from either the inside

or outside duct surface for the subject duct. As will be discussed later, the propulsion test included a large range of loadings, and the resulting forces undoubtedly reflected a flow that separated far forward of the duct trailing edge (T.E.), perhaps midchord, on the outside duct surface.

EFFICIENCY OF DUCT AND PROPELLER SYSTEM

The theoretical propulsive performance of the ducted propeller can be analyzed by using the thrust and power coefficients, which were computed from the propeller lifting-line programs discussed previously, and estimated hull efficiency factors. In terms of the section drag-to-lift ratio ϵ , the hydrodynamic pitch angle β_i , and the nonviscous propeller thrust and power coefficients, the viscous propeller thrust and power coefficients are:

$$C_{Ths} = \int_{x_h}^1 (1 - \epsilon \tan \beta_i) \frac{d(C_{Ths})_i}{dx} dx \quad (3)$$

$$C_{TP} = \int_{x_h}^1 (1 - w_x) (1 - \epsilon \tan \beta_i) \frac{d(C_{Ths})_i}{dx} dx \quad (4)$$

and

$$C_{Ps} = \int_{x_h}^1 \left(1 + \frac{\epsilon}{\tan \beta_i}\right) \frac{d(C_{Ps})_i}{dx} dx \quad (5)$$

The propeller wake-adapted propeller efficiency η_B is the ratio of the propeller-thrust power (output) to the propeller-absorbed power (input) and is given by

$$\eta_B = \frac{C_{TP}}{C_{Ps}} \quad (6)$$

Finally, the total efficiency of the duct plus propeller is

$$\eta_T = \eta_B \left(1 + \frac{T_d}{T_p}\right) \quad (7)$$

Figure 10 shows η_B versus model rpm as obtained from Equations (4), (5), and (6) with the total wake (hull plus duct) as input to the composite ducted-propeller computer program for the given propeller diameter and thrust-loading coefficient. It may be seen that optimum efficiency occurred at 800 rpm.

The quasi-propulsive coefficient is defined* as

$$\eta_D = \frac{P_E}{P_D} = \eta_T \cdot \eta_H \quad (8)$$

where

$$\eta_H = (1 - t) / (1 - w_0)$$

$1 - t$ is the thrust-deduction coefficient, and

$1 - w_0$ is the effective inflow-velocity ratio.

From data contained in Reference 4, $1 - t$ was estimated to be 0.88. If it is assumed that $(1 - w_0) \approx (1 - w_v)$ where the volume-mean inflow-velocity ratio is defined by

$$1 - w_v = \frac{2}{1 - x_h^2} \int_{x_h}^1 \frac{V_x}{V} x dx \quad (9)$$

then the hull efficiency η_H can be estimated by an integration of the curve of $(1 - w_x)$ total versus x given in Figure 6. A value $\eta_H = 0.88 / 0.823 = 1.07$ was obtained. The theoretically predicted quasi-propulsive coefficient for the final ducted propeller design may be calculated from the optimum value $\eta_B = 0.675$ (Figure 10 and Equations (7) and (8)). Thus,

$$\eta_D = 0.675 (1 + 0.04) 1.07 = 0.75$$

where the ratio T_d / T_p is taken as 0.04.

PROPULSION TEST RESULTS AND DISCUSSION

Figure 11 shows the results of the submerged overload and underload propulsion test of NSRDC Model 4620 with the duct and Propeller 4271. From the experimental curves of Figure 11, it is possible to analyze and to compare the powering performance of the cruising, ducted-propeller system to its theoretically predicted performance and to the performance of an optimum wake-adapted, unducted stern propeller.

Two generally recognized approaches were considered for interpreting the results of the resistance and propulsion tests. On the one hand, the towed resistance could be taken as the bare hull and the propulsor could be viewed as the complete duct and propeller unit. On the other hand, the towed resistance could consist of the hull plus duct without propeller. In the latter case, the duct would be viewed as an appendage to the hull. Both approaches, of course, would lead to the same prediction of shp and rpm for the prototype. However, in the present case, the author preferred to include the duct in the towed resistance because it is easier to compare theory and experiment.

*The drag is defined as the hull plus duct with the various propulsion quantities estimated as indicated.

Table 3 and Figure 12 give the pertinent data for powering a 200-ft prototype of Model 4620 with a correlation-allowance coefficient $\Delta C_f = 0.5 \times 10^{-3}$. The data of Table 3 are given for a constant ship speed. However, the various propulsion coefficients are essentially constant over a wide range of ship speed; $V = 29.3$ knots follows from the design condition. It is found from the shp given in Table 3 that the ducted propeller absorbs about 28 percent more power than does the unducted optimum single-screw propeller. The percentage applies over the entire submerged-speed range. The relatively low efficiency of the ducted propeller is due in part to its smaller diameter and higher rpm, and to the zero value of T_d/T_p at ship propulsion.

TABLE 3

Comparative Propulsion Data for a 200-Foot Prototype
of Model 4620 at $V = 29.3$ Knots

($10^3 \Delta C_f = 0.5$; propellers at Station $x = 0.966$)

Quantity	Estimated Optimum Single-Screw Propeller [†] ($D_p = 13.63$ ft $Z = 5$)	Ducted Propeller ($D_p = 10.04$ ft** $Z = 7$)		
		Theoretical (Predicted)	Experimental (Actual)	Experimental at (C_{Ths}) Design
RPM	150	220 (optimum)	237	233
SHP	7000	8900	8990	8936
J_s	1.45	1.344	1.246	1.267
C_{Ths}	0.233	0.400**	0.423	0.400
T_d/T_p		0.039	0.00	-0.046
η_T		0.70	0.67	0.66
η_B	0.77	0.675	0.67	0.69
η_D^{***}	0.85	0.75	0.74	0.747
η_H	1.11	1.07	1.11	1.14
$(1-t)_p$ or $(1-t)_{tot}$	0.86	0.88	0.912	0.943
$(1-w_0)$ See Equation (9)	0.79	0.823	0.823	0.823

*From Reference 4.
**From Reference 1.
*** η_D Cannot be compared for single screw and ducted propeller because P_E is different.
D Comparison should be based on shp.

As mentioned previously, the limited objective of the present work was to evaluate the ducted propeller configuration developed in Reference 1. For the wake-adapted case, the best propeller is not necessarily that with the largest practical diameter. To optimize on the basis of minimum shp, the variation of the hull efficiency with propeller diameter must be considered. It is very likely that improved performance could be expected for the present ducted propeller if a larger diameter (probably close to that for the optimum unducted propeller) were chosen. An estimate indicated that the predicted 4-percent duct thrust would probably be lost in overcoming the drag of the four supporting struts, which was not considered in the theory.

In attempt to further explain the 28 percent more power required by the present ducted propeller than by an unducted optimum single-screw propeller, propulsive performance was examined for other apparently successful ducted-propeller configurations.¹² It was found that the usual cruciform-stern-appendage arrangement for submarines could increase hull efficiency by about 3 percent. The configurations examined had utilized stator vanes, and calculations showed that their use with the subject ducted propeller could improve total efficiency by more than 5 percent. These factors, combined with the stringent circumstance of comparing with an *optimum* unducted propeller, go far in explaining the relative propulsive performance. It seems likely from the foregoing that an improved cruising-ducted propeller could be developed with performance perhaps comparable with existing designs.

It is important to compare the theoretically predicted ($J_s = 1.344$) and experimental ($J_s = 1.267$) performances of the ducted propeller (Table 3) at the design thrust-loading coefficient $C_{Ths} = 0.400$. In analyzing this result, it was found that the propeller was under-pitched due to an error in input to one of the computer programs and, therefore, that it operated at a rpm that was about 6 percent high. Performance at ship propulsion might have been better had the required thrust been known more accurately. In the design process¹ model boundary-layer characteristics were used, and a ship-model correlation allowance was not considered. It is seen that at design C_{Ths} the theoretical and experimental values of shp were 8900 and 8936, respectively.

Two features of the performance of the present ducted propeller at unusually high overload (about three times C_t for the ship) are worthy of comment:

1. $K_{T_{total}}$ increased almost linearly in the high range of C_t , and the duct thrust was approximately 40 percent of the propeller thrust.
2. Although considerable thrust was carried by the duct, this portion of the total thrust was not delivered effectively to the hull as indicated by the decreasing total thrust-deduction factor $(1-t)_{total}$. The fact that the loaded duct augmented the hull drag relatively more than did the propeller load may be due to the fact that the center of thrust on the duct shifted forward at large overloads.

CONCLUSIONS

1. Agreement was good for the theoretical pressure distribution on the *outside* of the duct as calculated by the present method and that of Kriebel and Mendenhall¹ for a duct of zero thickness. Agreement was not as good for the pressure distribution on the *inside* of the duct.

2. The theoretically predicted shp was within 1 percent of the experimental shp. The experimental propeller rpm was 6 percent higher than the design value because the propeller was underpitched.

3. A 200-ft prototype equipped with the cruising, ducted-propeller unit required 28 percent more shp than did a conventional unshrouded optimum single-screw over the entire speed range. The ducted propeller performance could be improved by a parametric study to determine the optimum propeller rpm-diameter relationship and other design refinements.

4. At high overload, the duct thrust was about 40 percent of the propeller thrust; however, the thrust was not effectively delivered to the hull as indicated by the decreasing total thrust-deduction factor.

ACKNOWLEDGMENTS

The author expresses his thanks to Messrs. A. Weaver, J. Nelka, and N. Oliver of the Ship Powering Division for conducting the experiments.

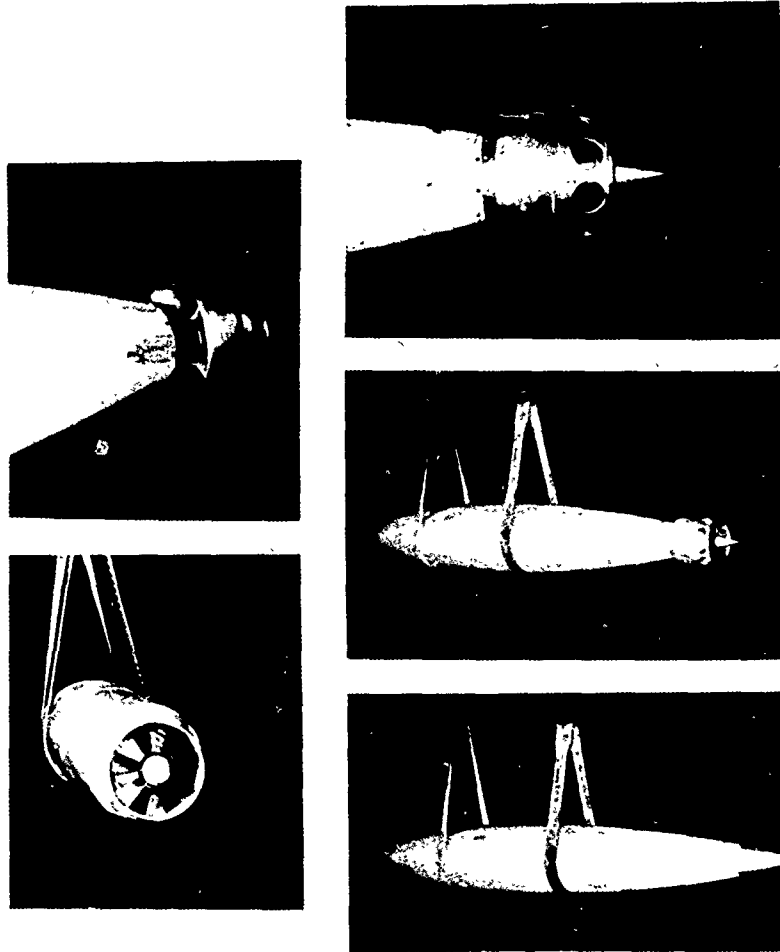


Figure 1 – NSRDC Model 4620 with Ducted Propeller 4271

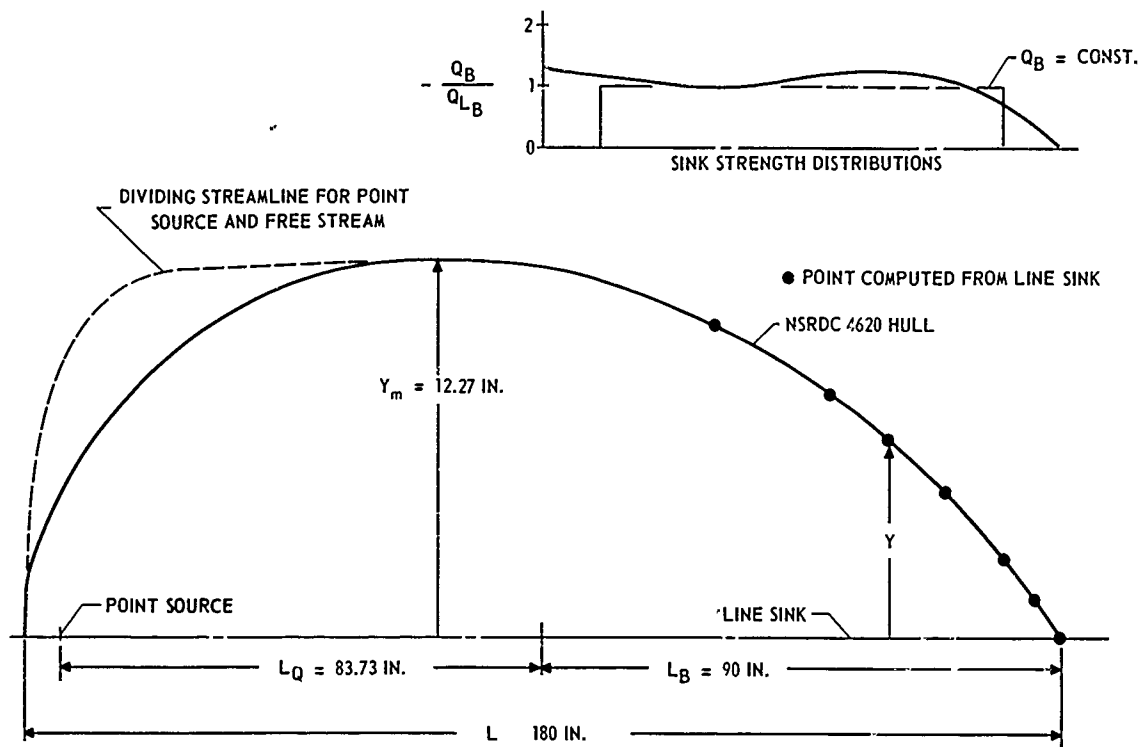


Figure 2 – Comparison of Hull Shapes for NSRDC Model 4620 and for the Point Source and Line Sink of Reference 1



Figure 3 – Cruising Duct 2.1

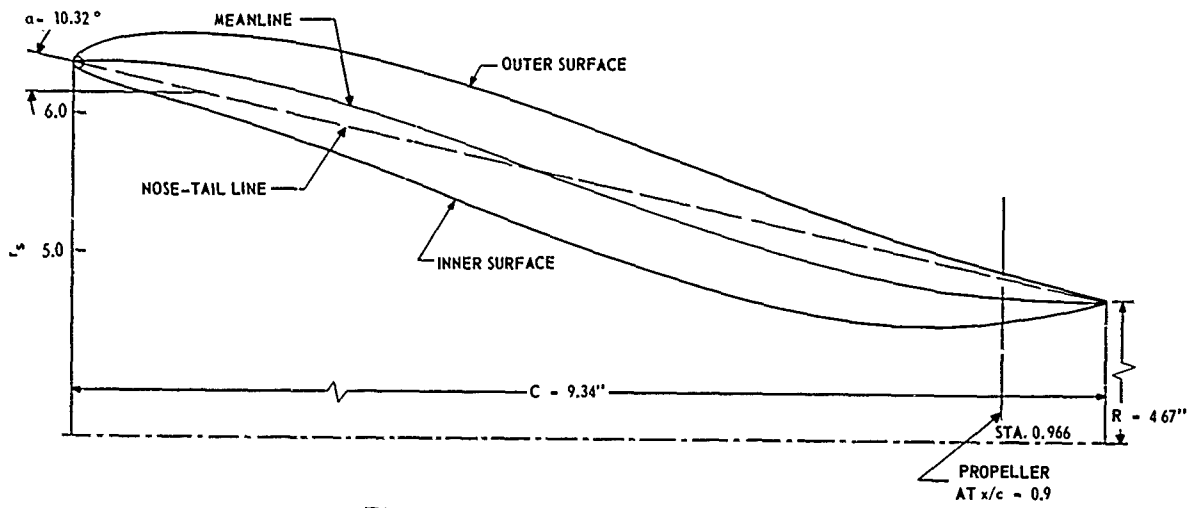


Figure 4 - Duct Section and Dimensions

NUMBER OF BLADES	7
EXPANDED AREA RATIO	0.500
MWR	0.176
BTF	0.027
P/D (AT 0.7R)	1.333
DIAMETER	9.040 IN.
PITCH (AT 0.7R)	12.050 IN.
ROTATION	R.H.

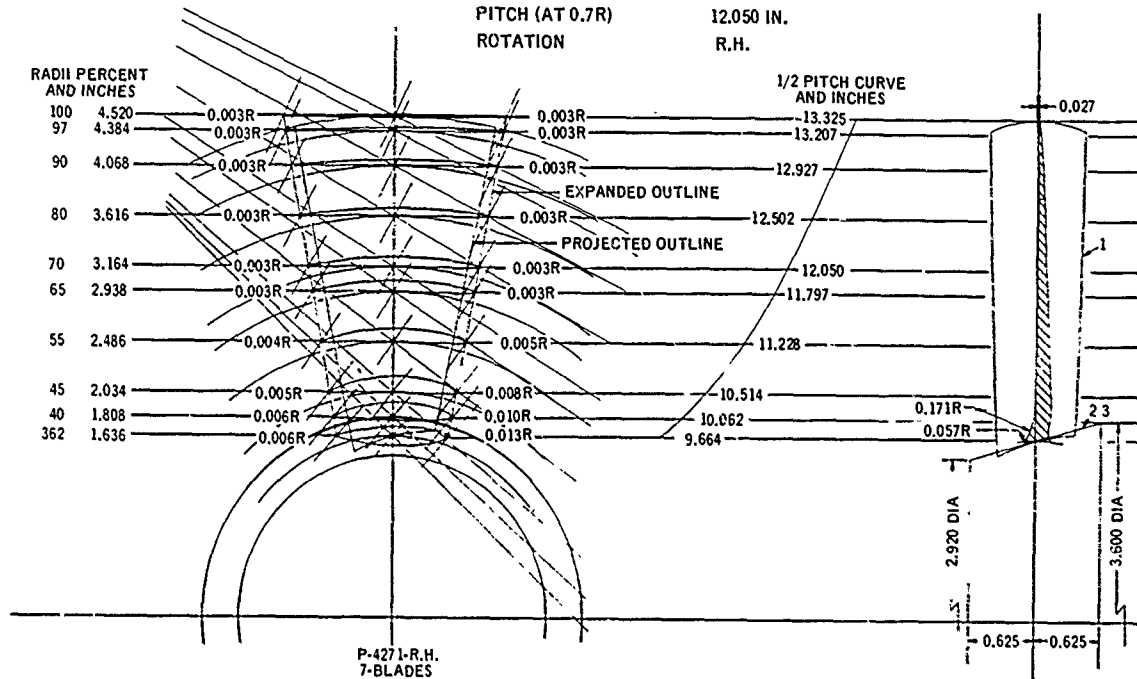


Figure 5 - Details of Propeller 4271

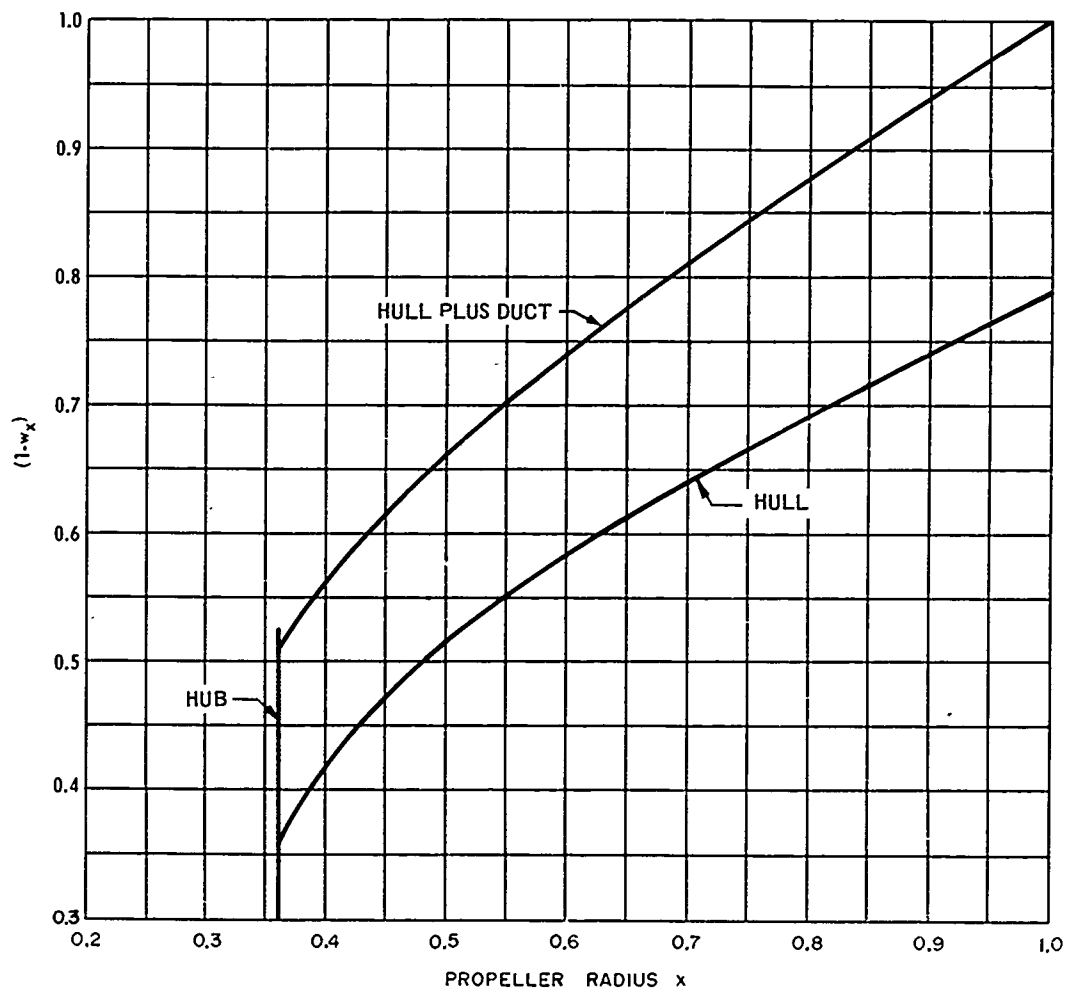


Figure 6 - Hull Wake and Total Wake of Hull Plus Duct

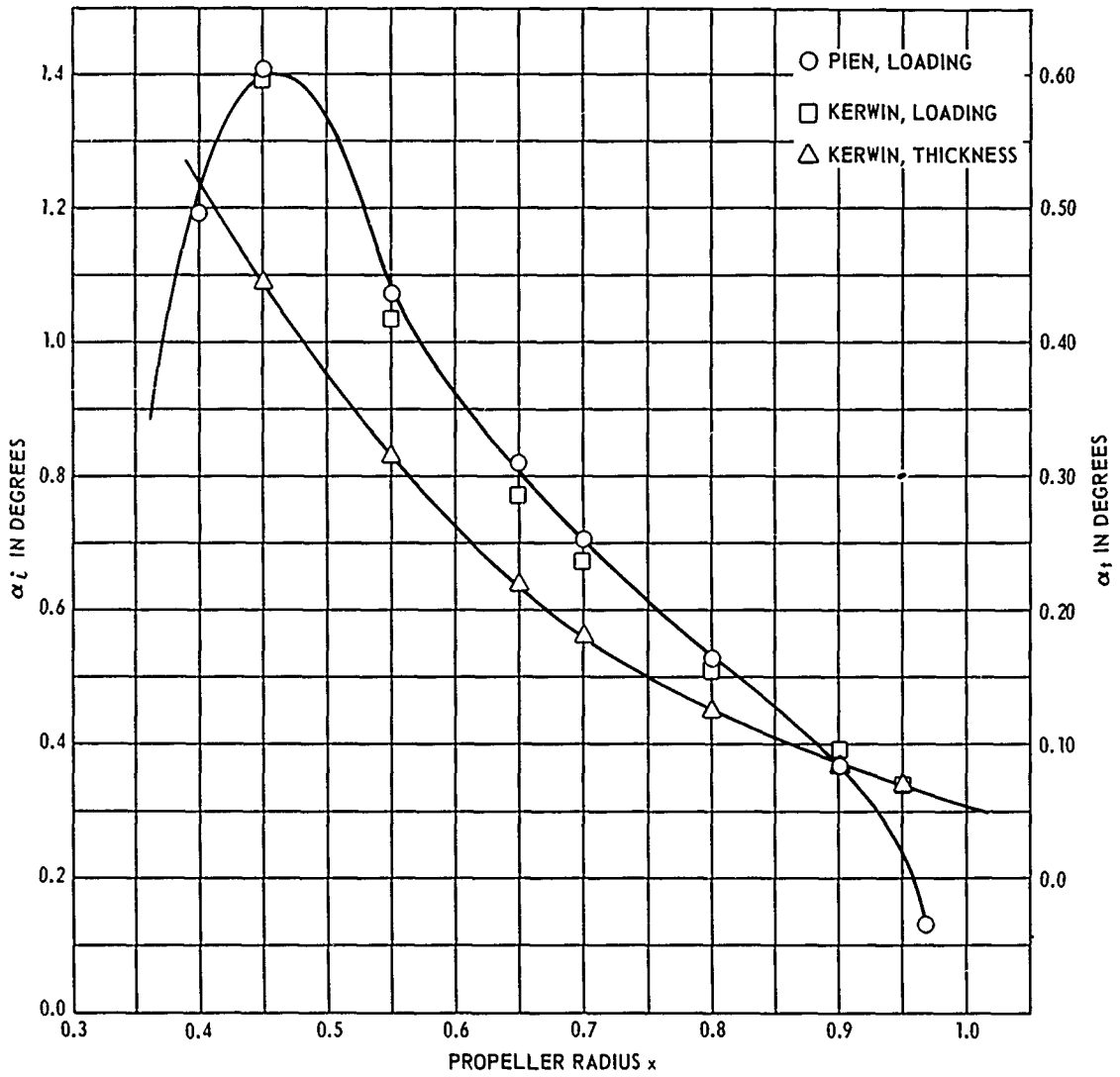


Figure 7 - Additional Angles of Attack for Blade Sections of Propeller 4271

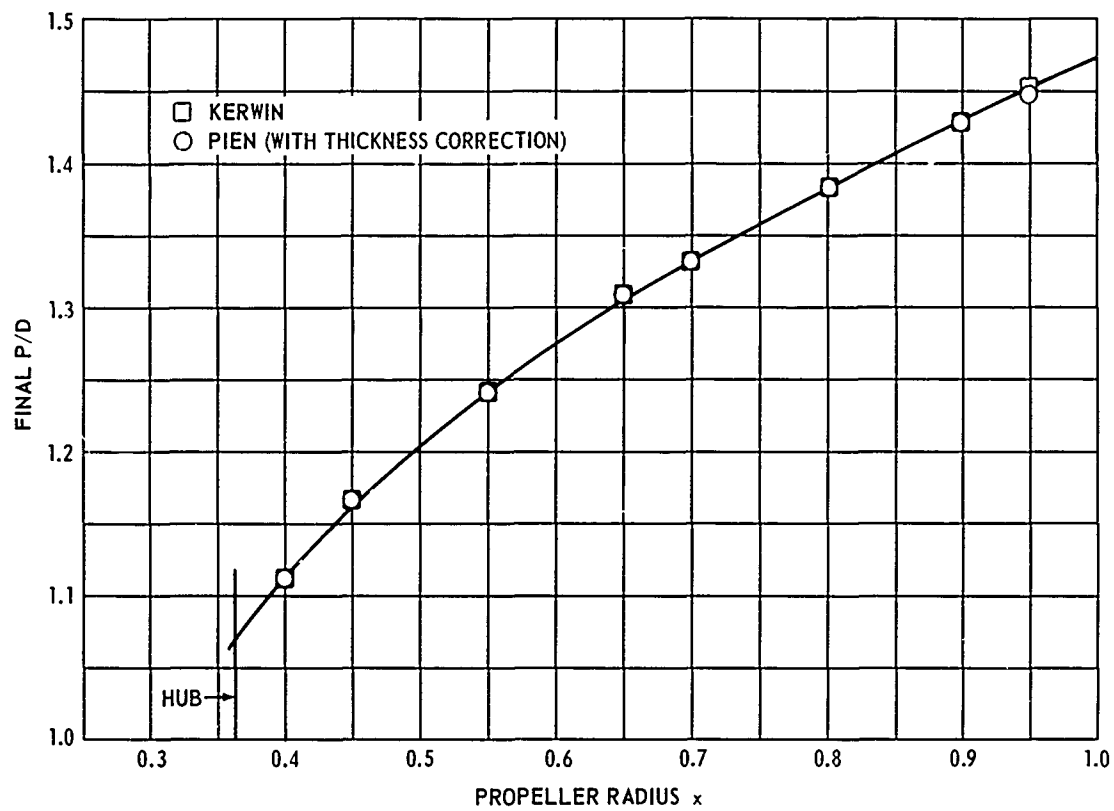


Figure 8 - Final Blade-Pitch Distribution for Propeller 4271

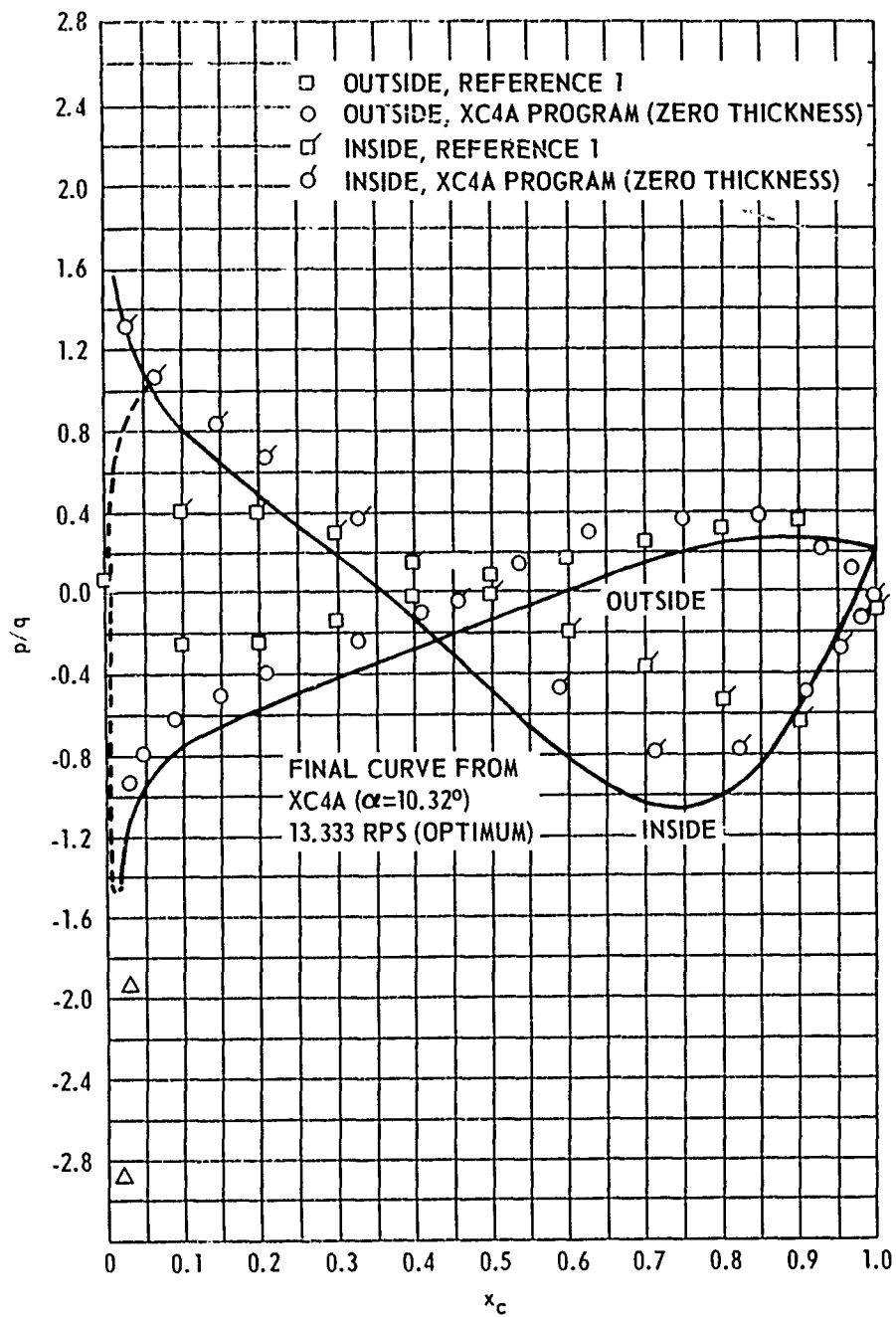


Figure 9 - Pressure Distribution on Duct

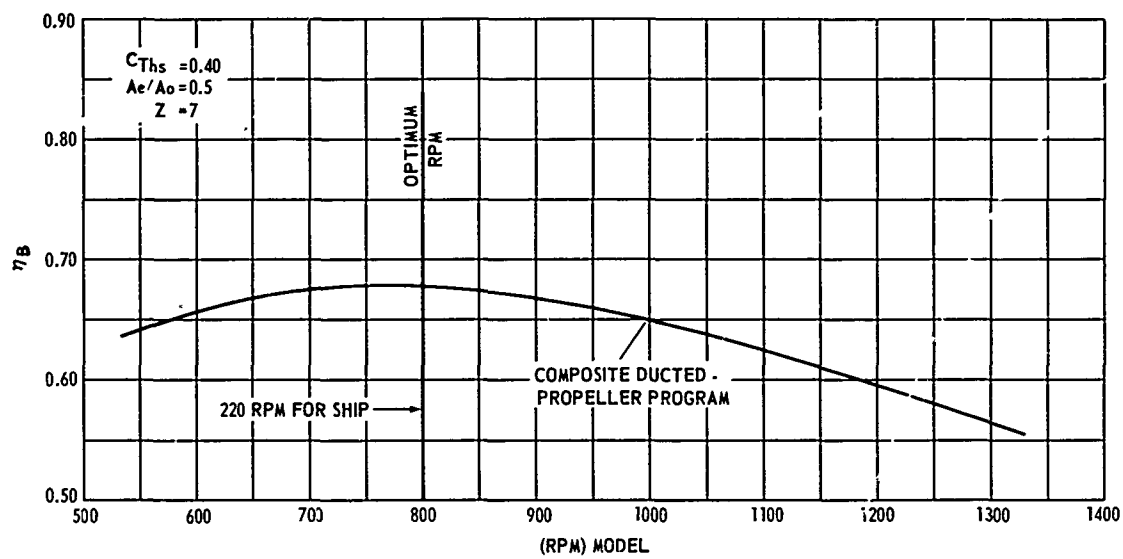


Figure 10 – Ducted Propeller Efficiencies versus RPM

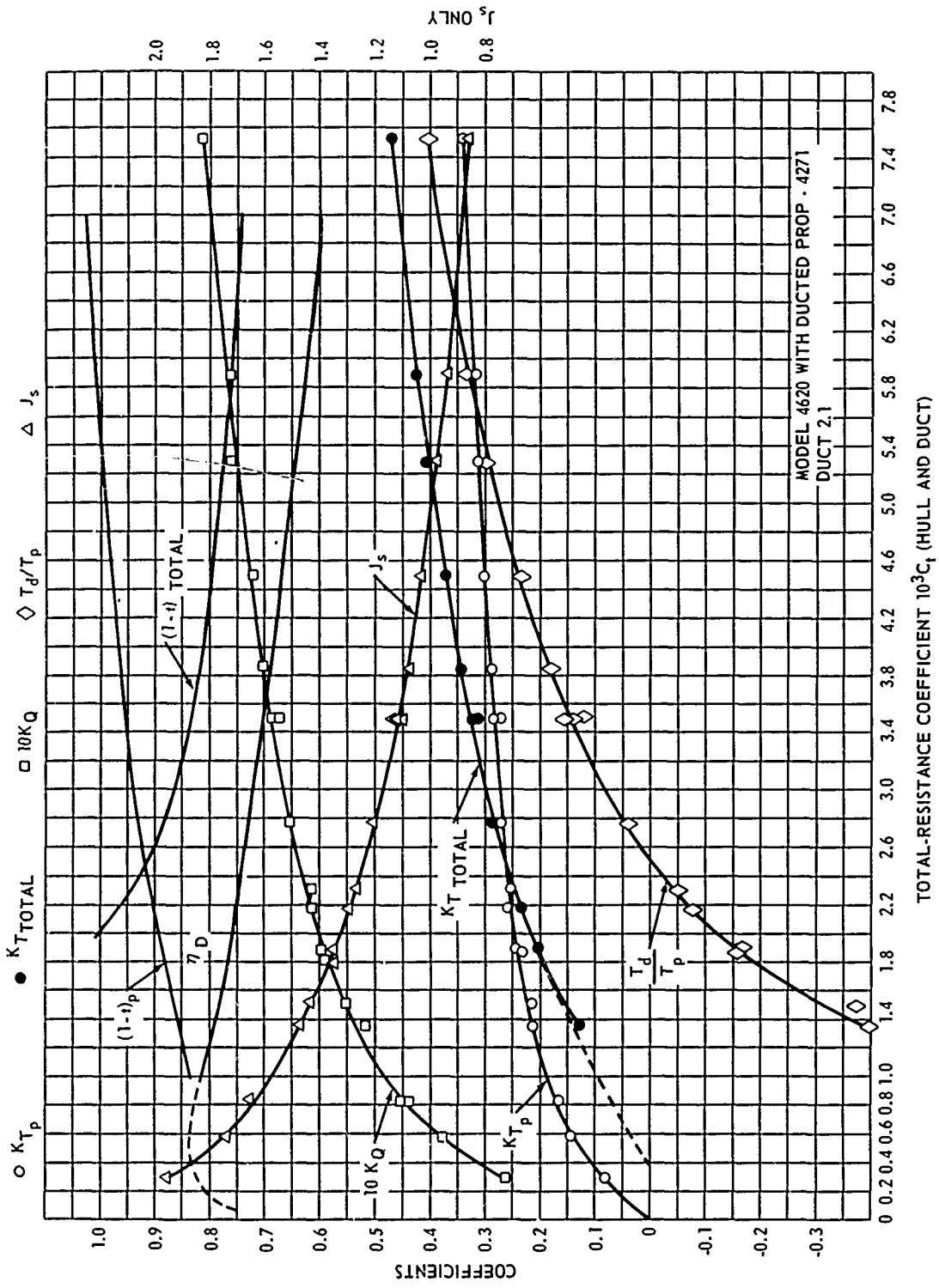


Figure 11 — Model 4620 Overload and Underload Propulsion with Ducted Propeller 4271

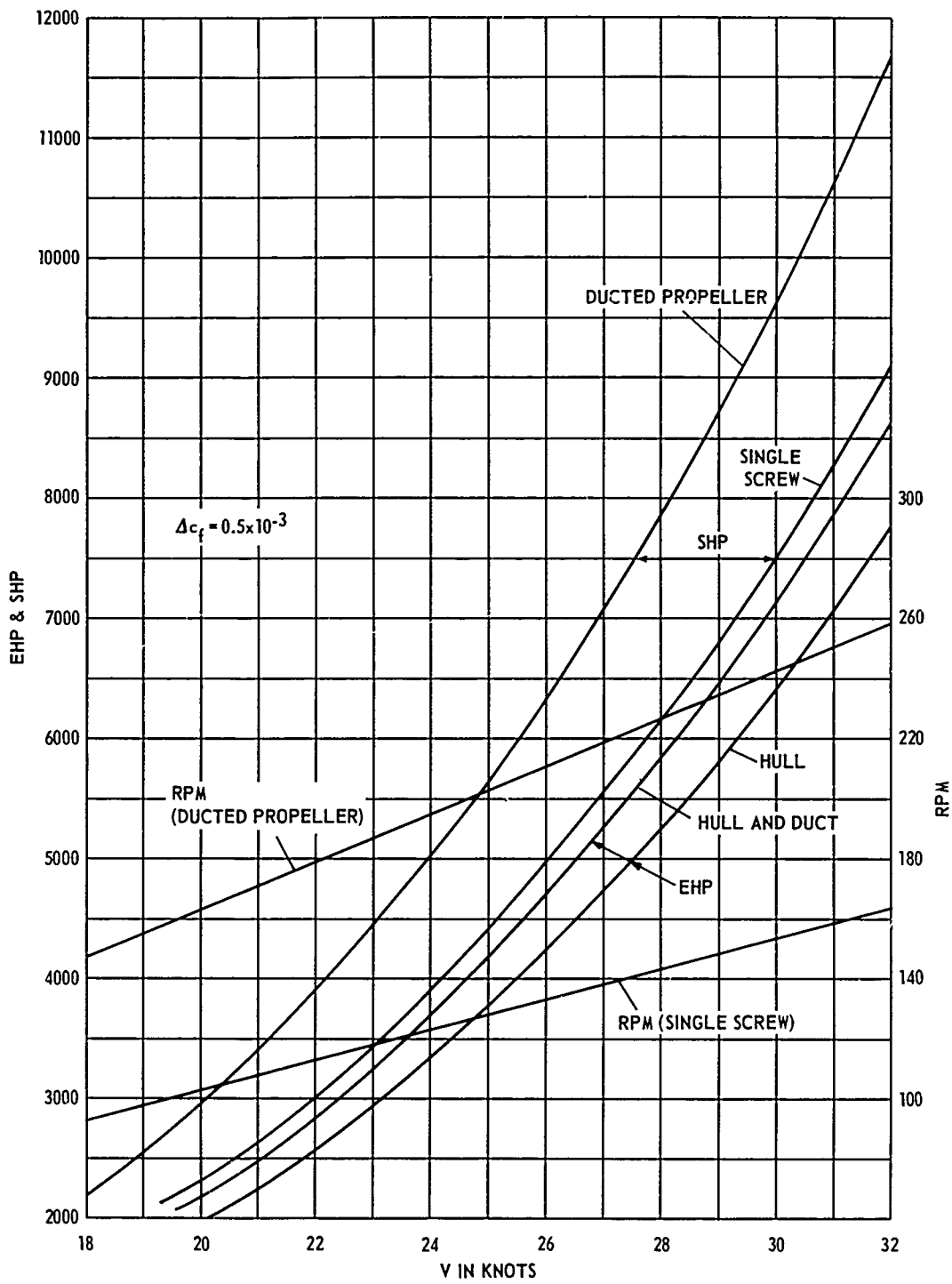


Figure 12 – Power and RPM Curves for a 200-Foot Prototype of Model 4620

REFERENCES

1. Kriebel, A.R. and Mendenhall, M.R., "Interference between a Hull and a Stern-Mounted Ducted Propeller," VIDYA, Division of Itek Corp., Report 204, Contract Nonr-4278(00) (30 Oct 1965).
2. Morgan, W.B., "A Theory of the Ducted Propeller with a Finite Number of Blades," Institute of Engineering Research, University of California, Berkeley (May 1961).
3. Caster, E.B., "A Computer Program for Use in Designing Ducted Propellers," NSRDC Report 2507 (Oct 1967).
4. Beveridge, J.L., "Effect of Axial Position of Propeller on the Propulsion Characteristics of a Submerged Body of Revolution," David Taylor Model Basin Report 1456 (Mar 1963).
5. Morgan, W.B., and Caster, E.B., "Prediction of the Aerodynamic Characteristics of Annular Airfoils," NSRDC Report 1830 (Jan 1965).
6. Lerbs, H.W., "Moderately Loaded Propellers with a Finite Number of Blades and an Arbitrary Distribution of Circulation," Transactions, Society of Naval Architects and Marine Engineers, Vol. 60 (1952).
7. Hough, G.R. and Ordway, D.E., "The Generalized Actuator Disk," Advanced Research Report TAR-TR6401, Therm, Inc. (Jan 1964).
8. Haskins, E.W., "Calculation of Design Data for Moderately Loaded Marine Propellers by Means of Induction Factors," NSRDC Report 2380 (Sep 1967).
9. Cheng, H.M., "Hydrodynamic Aspect of Propeller Design Based on Lifting-Surface Theory, Part 2 - Arbitrary Chordwise Load Distribution," David Taylor Model Basin Report 1803 (Jun 1965).
10. Kerwin, J.E., and Leopold, R., "Propeller Incidence Correction Due to Blade Thickness," Journal of Ship Research, Vol. 7, No. 2 (Oct 1963).
11. Pien, P.C., "The Calculation of Marine Propellers Based on Lifting Surface Theory," Journal of Ship Research, Vol. 5, No. 2 (Sep 1964).

UNCLASSIFIED

Security Classification

DOCUMENT CONTROL DATA - R & D

(Security classification of title, body of abstract and indexing annotation must be entered when the overall report is classified)

1. ORIGINATING ACTIVITY (Corporate Author) Naval Ship Research and Development Center Washington, D.C. 20034		2a. REPORT SECURITY CLASSIFICATION UNCLASSIFIED	
		2b. GROUP	
3. REPORT TITLE HYDRODYNAMIC PERFORMANCE OF A PROPOSED CRUISING, DUCTED PROPELLER FOR SUBMARINES			
4. DESCRIPTIVE NOTES (Type of report and inclusive dates)			
5. AUTHOR(S) (First name, middle initial, last name) John L. Beveridge			
6. REPORT DATE April 1971		7a. TOTAL NO. OF PAGES 28	7b. NO. OF REFS 12
8a. CONTRACT OR GRANT NO.		9a. ORIGINATOR'S REPORT NUMBER(S) Report 3374	
b. PROJECT NO. SR 009 0101 Task 0101		9b. OTHER REPORT NO(S) (Any other numbers that may be assigned this report)	
c.			
d.			
10. DISTRIBUTION STATEMENT Distribution limited to U.S. Government agencies only; Test and Evaluation; 28 Nov 1970. Other requests for this document must be referred to NSRDC, Code 500.			
11. SUPPLEMENTARY NOTES		12. SPONSORING MILITARY ACTIVITY Naval Ship Systems Command	
13. ABSTRACT <p>A theoretical and experimental investigation was performed to determine the steady-state propulsion characteristics of a cruising, ducted-propeller system for a submersible body of revolution. The most important aspects of the design method and numerical procedures are discussed. The theoretically predicted and experimental performance of the ducted propeller showed good agreement on power. However the experimental rpm was 6 percent higher than predicted; this difference is attributed to the fact that the propeller was underpitched due to an error in input to the computer program. The subject propulsion system was found to be less efficient than an optimum unshrouded, wake-adapted propeller, but the optimum rpm-diameter relationship was not determined for the ducted propeller.</p>			

UNCLASSIFIED

Security Classification

14. KEY WORDS	LINK A		LINK B		LINK C	
	ROLE	WT	ROLE	WT	ROLE	WT
Ducted Propeller Design Ducted Propeller Performance Submarine Propulsion						

UNCLASSIFIED

Security Classification